RESEARCH ARTICLE

Proteomic analysis of lipid body from the alkenone-producing marine haptophyte alga *Tisochrysis lutea*

Qing Shi[1], Hiroya Araie[2,3], Ranjith Kumar Bakku[1], Yoichiro Fukao[4], Randeep Rakwal[5], Iwane Suzuki[2,3] and Yoshihiro Shiraiwa[2,3]

[1] Graduate School of Life and Environmental Sciences, University of Tsukuba, Tennodai, Tsukuba, Ibaraki, Japan
[2] Faculty of Life and Environmental Sciences, University of Tsukuba, Tennodai, Tsukuba, Ibaraki, Japan
[3] CREST, JST, Tennodai, Tsukuba, Ibaraki, Japan
[4] Plant Global Educational Project, Nara Institute of Science and Technology, Ikoma, Japan
[5] Organization for Educational Initiatives, University of Tsukuba, Tennodai, Tsukuba, Ibaraki, Japan

Lipid body (LB) is recognized as the cellular carbon and energy storage organelle in many organisms. LBs have been observed in the marine haptophyte alga *Tisochrysis lutea* that produces special lipids such as long-chain (C_{37}-C_{40}) ketones (alkenones) with 2–4 *trans*-type double bonds. In this study, we succeeded in developing a modified method to isolate LB from *T. lutea*. Purity of isolated LBs was confirmed by the absence of chlorophyll auto-fluorescence and no contamination of the most abundant cellular protein ribulose-1,5-bisphosphate carboxylase/oxygenase. As alkenones predominated in the LB by GC-MS analysis, the LB can be more appropriately named as "alkenone body (AB)." Extracted AB-containing proteins were analyzed by the combination of 1DE (SDS-PAGE) and MS/MS for confident protein identification and annotated using BLAST tools at National Center for Biotechnology Information. Totally 514 proteins were identified at the maximum. The homology search identified three major proteins, V-ATPase, a hypothetical protein EMIHUDRAFT_465517 found in other alkenone-producing haptophytes, and a lipid raft-associated SPFH domain-containing protein. Our data suggest that AB of *T. lutera* is surrounded by a lipid membrane originating from either the ER or the ER-derived four layer-envelopes chloroplast and function as the storage site of alkenones and alkenes.

Received: January 8, 2015
Revised: March 2, 2015
Accepted: April 23, 2015

Keywords:
Alkenone body / Haptophyte / Lipid body / Proteome / *Tisochrysis lutea*

Additional supporting information may be found in the online version of this article at the publisher's web-site

1 Introduction

Marine haptophyte algae are known to be globally distributed as one of the greatest producers of biomass in the ocean [1]. Haptophytes comprise both calcifying species, called coccolithophores, and noncalcifying species. *Emiliania huxleyi* (Isochrysidales) is one of the cosmopolitan species of coccolithophores and known to produce huge blooms that are often observed from satellite such as SeaWiFs especially at high latitude oceans [2]. Therefore, *E. huxleyi* is regarded as an important player in transporting atmospheric CO_2 to the ocean sediment as calcium carbonate and organic matter by

Correspondence: Dr. Yoshihiro Shiraiwa, Faculty of Life and Environmental Sciences, University of Tsukuba, 1-1-1 Tennodai, Tsukuba, Ibaraki 305–8572, Japan
E-mail: emilhux@biol.tsukuba.ac.jp
Fax: +81-29-853-6614

Abbreviations: **AB**, alkenone body; **LB**, lipid body; **LDSP**, lipid droplet surface protein; **MLDP**, major lipid droplet protein; **PNS**, postnuclear supernatant; **RuBisCO**, ribulose-1,5-bisphosphate carboxylase/oxygenase; **SDR**, short-chain dehydrogenase reductase; **TAG**, triacylglycerol

functioning as the biological pump. On the other hand, a noncalcareous marine haptophyte species *Tisochrysis lutea*, previously named as *Isochrysis* aff. *galbana* (Clone Tahiti) as a taxonomic variation of *Isochrysis* species [3], not known as bloom-producing alga in the ocean has been well studied in aquaculture research for its mass cultivation as commercial feed for fish [4, 5]. In particular, lipids of *T. lutea* are used as a suitable nutrition source for the larvae due to the presence of high amounts of long-chain polyunsaturated fatty acids such as docosahexaenoic acid [6, 7].

Interestingly, most of the species in Isochrysidales also produce unique neutral lipid molecules of long-chain ketones, called alkenones [8–10], instead of the universally stored glycerolipids such as triacylglycerol (TAG). Alkenones have been identified as the major neutral lipids in *T. lutea* [10]. Alkenones are typical in their carbon chain length (from C_{37} to C_{40}) and carry two to four *trans*-type double bonds and one *keto*-group [11]. So far, only five strains of haptophytes in the order Isochrysidales are known to produce alkenones [10, 12]. The number of unsaturated bonds in a molecule of alkenone is known to increase when cells are grown or maintained at low temperature. Because of this, alkenones have been widely used as biomarkers for the reconstruction of marine paleo-temperature by determining the unsaturation index, $U^{K'}_{37}$, calculated as a parameter of the ratio of $C_{37:2}$ to $C_{37:3}$ alkenones [13, 14]. Previous studies have suggested that alkenones are stored in organelles known as lipid bodies (LBs) and function as a storage lipid in the cells [7, 15]. According to geological survey, alkenones are regarded as one of the sources for petroleum generated in geological history such as in the Cretaceous era [8, 16, 17]. As such, alkenones have garnered broad interests in geological, biological, and industrial fields, but the cellular machinery and metabolic process for their production remained largely unknown [18–20].

LBs widely existing in eukaryotic cells are generally believed to be the storage center of TAG [21, 22]. Recent studies of TAG-producing LBs, however, have revealed that LBs might also serve as a storage organelle for endogenous proteins, and that these proteins carry diverse functions in lipid metabolism, cell signaling, intracellular trafficking, and protection against pathogen infection [23–30]. It is generally accepted that oleosins and caleosins function as structural proteins in LBs of higher plants while steroleosins appears to play a role in signal transduction [31–33]. Also, in seed oil bodies of *Arabidopsis thaliana*, a member of the short-chain steroid dehydrogenase reductase superfamily was identified although its function remains unknown [34].

In the green alga *Chlamydomonas reinhardtii*, the major lipid droplet protein (MLDP) was shown to be a structural protein of LBs [35, 36]. MLDP was also found in the salt-tolerant green alga *Dunaliella* sp. [37]. Others examples are a *Haematococcus* oil globule protein in *Haematococcus pluvialis* [38], a primitive caleosin in *Chlorella* sp. [39], and a lipid droplet surface protein (LDSP) in *Nannochloropsis* sp. [40, 41].

It is commonly assumed that LBs in higher plants are likely to be formed by budding from the ER [41]; while in microalgae such as *C. reinhardtii* [42] and *T. lutea* the location where LBs arise from is still a mystery. Glycerol-3-phosphate acyltransferase MmGPAT3, lysophosphatidic acid acyltransferase, and phospholipid/diacylglycerol acyltransferase were detected in LBs of *C. reinhardtii* [36] and therefore are very likely related to oil biosynthesis. This kind of information can help to interpret lipid metabolism in LBs. However, LBs in alkenone-producing, but no or very low amounts of TAG, organisms as well as the secondary symbiotic organisms have not yet been properly characterized. Moreover, the mechanism of LB formation including site information is virtually unknown. Revealing the proteins associated with LBs in the marine haptophyte *T. lutea* can provide new insights on where and how these alkenone-dominant LBs are formed in addition to understanding alkenone metabolism. Furthermore, the LB proteome might aid in exploring the unique features of LBs and the lipid production mechanism in non-TAG-producing organisms.

In this present study, our focus is three-fold: (i) establishment of a protocol for the isolation and purification of LBs from the haptophyte *T. lutea*, (ii) analysis of lipid composition in the purified LBs, and (iii) proteomic analysis of the purified LBs. Briefly, the LBs were isolated and purified by a newly developed method that utilized a sucrose density gradient centrifugation with stepwise sucrose density layers, followed by their purity check and proteomic analysis using 1DE (SDS-PAGE) linked to tandem mass spectrometry to reveal the LB proteins. To our knowledge, this report is the first inventory of *T. lutea* LB proteome, which could serve as a resource for researchers studying alkenone producing algae including lipid metabolism and biofuel production since alkenones are one of important candidates for the production of algal biofuels [43].

2 Materials and methods

2.1 Organism and culture conditions

The haptophyte alga *Isochrysis* aff. *galbana* (Clone Tahiti) (also referred to as T-iso) examined in this study, and which was recently renamed as *Tisochrysis lutea* [3], was obtained from the Matsunaga laboratory, Tokyo University of Agriculture and Technology. This strain has been maintained in our laboratory for around 15 years. The cells were grown in a 20 L polycarbonate carboy (Nalgene) containing artificial seawater, Marine Art SF-1 (Tomita Seiyaku Co., Ltd., Tokyo, Japan) enriched with the Erd–Schreiber's medium (MA-ESM), and soil extracts that were replaced by 10 nM sodium selenite [44]. The MA-ESM also contains 1.4 mM sodium nitrate (120 mg/L). Salinity of the medium was modulated to 30‰ using a Refractometer (MASTER-S/MillM, ATAGO Co. Ltd., Tokyo, Japan) before adding ESM and sodium selenite. Cells used for the experiments were grown at 20°C for 2 weeks until they reached stationary growth phase. We used RQflex Plus Reflectometer (Merck, Darmstadt, Germany) with

Reflectoquant (Test Strip) for nitrate test (Merck) in a separate experiment under same condition (unpublished data). For nitrogen-deficient culture, cells were transferred to nitrogen-depleted medium lacking sodium nitrate (−N medium) after washing once with −N medium by centrifugation (5 min at 4000 × *g*). Cells were separated into six oblong glass vessels after resuspension into −N medium and then grown under constant illumination (100 μmol photons m^{-2} s^{-1}) and aeration (100 mL/min) at 20°C for about 2 weeks.

2.2 Lipid body isolation

The protocol for isolation of LB was established with reference to a previous study [45]. We briefly describe this modified protocol. The algal cells were harvested by centrifugation (5 min at 4000 × *g*) from 40 L of algal culture and the resultant cell pellet was resuspended into 10 mM sodium phosphate buffer (pH 7.5) with 0.25 M sucrose and protease inhibitor cocktail (ProteoGuard™ EDTA-free protease inhibitor cocktail, Clontech, CA, USA). The cells were placed on ice for 15 min and then broken by a French Press with 0.8 kpsi at 4°C. To remove some debris, cell lysates were centrifuged at 3000 × *g* for 10 min at 4°C. After centrifugation, a large amount of LBs was obtained in the supernatant fraction, called postnuclear supernatant (PNS), as described in the Nature protocol [45]. Sucrose concentration in the PNS sample was adjusted to 1 M. Then, the sample was applied to a centrifuge tube containing layers of 1.2, 1.0, 0.8, 0.5, 0.25, and 0 M sucrose for a sucrose stepwise gradient centrifugation for 30 min at 10 000 × *g* (SW40 Ti rotor, Beckman Coulter, CA, USA) at 4°C. LBs fractionated onto the top layer was carefully collected by a pipette and then transferred to a new 1.5 mL Eppendorf tube. The crude LB fraction was washed three times with 10 mM sodium phosphate buffer (pH 7.5) followed by centrifugation for 10 min at 10 000 × *g* at the bottom (12 000 rpm using TMP-21 rotor of TOMY MX-201 and a ARO15-24 of TOMY MX-307 minirefrigerator centrifuge, TOMY, Japan) to remove contaminants of other organelles, cytosolic proteins, and other materials.

2.3 BODIPY staining

BODIPY (493/503, Life Technologies, CA, USA) stock solution was prepared as 1 mg/mL in dimethyl sulfoxide. The staining was carried out by mixing with algal culture or isolated LBs in order to observe LBs in the living cells under a fluorescent microscope (BX50, Olympus, Japan).

2.4 Analysis of lipid composition in LBs

The extraction of lipids was performed by following a previous protocol [45]. Extracted neutral lipids and methyl-esterified polar lipids were detected by an FID-equipped capillary gas chromatograph (GC-2014AFSC; Shimadzu, Kyoto, Japan) with a CP-SIL 5CB column (50 m, 0.32 mm id, 0.12 μm; Agilent, Santa Clara, CA, USA). The carrier gas used was He with a flow rate of 2.08 mL/min in split-less mode. The column temperature was set to 60°C for 1.5 min, heated at a speed of 20°C/min to 130°C, and then taken at 4°C min^{-1} to 300°C, and holding at 300°C for 25 min. Then composition of unknown peaks were analyzed by gas-chromatograph, GC-2010, equipped with a mass spectrometer, QP-2010 (Shimadzu, Kyoto, Japan) by following our previous method [47]. We identified these unknown peaks from the retention times and mass spectrums by using similarity search. Five micrograms heptadecanoic acid (17:0) and n-toriacontane (C_{30}) dissolved in hexane was added to each sample as internal standard.

2.5 Protein extraction

The proteins of isolated LBs were extracted using two methods. One method involved treatment with 90% acetone (Wako, proteomics grade, Osaka, Japan) for 16 h followed by centrifugation for 10 min at 12 000 × *g* (15000 rpm; TMP-21 rotor of TOMY MX-201 and a ARO15-24 of TOMY MX-307 minirefrigerator centrifuge, TOMY, Tokyo, Japan). After discarding the supernatant, precipitated proteins were treated with 90% acetone for another 16 h (preparation: AB1). The other method involved treatment with petroleum ether according to the methods of Katavic et al. [46] in which neutral lipids and polar lipids were extracted first (preparation: AB2). PNS samples were prepared from cells grown under N-deficient conditions (PNS/-N) and N-sufficient (standard) conditions (PNS/+N as control). Proteins were prepared from both PNS samples by 90% acetone precipitation and petroleum ether, according to the method described above. Precipitated proteins were dissolved in lysis buffer containing thiourea and tris [7 M w/v urea, 2 M w/v thiourea, 4% w/v CHAPS, 18 mM w/v Tris-HCl pH 8.0, 14 mM w/v Trizma base, 0.2% v/v triton X-100, 50 mM w/v DTT, 1% v/v pH 3–10 ampholyte, and two EDTA-free proteinase inhibitor (Roche Diagnostics GmbH, Tokyo, Japan), 1% v/v pharmalyte pH 3–10 and 50 mM DTT] [48]. Proteins were denatured by adding a SDS-containing sample buffer containing 62 mM Tris pH 6.8, 10% v/v glycerol, 2.5% w/v SDS, 5% v/v 2-mercaptoethanol (pH 6.8 with HCl) and 0.004% bromophenol blue [sample/buffer = 1/1 v/v] at 65°C for 10 min. Proteins were analyzed by SDS–PAGE on 12.5% gel w/v and visualized using OLEO™ fluorescent gel stain (Bio-Rad Laboratories, Inc., CA, USA). The protein concentration of samples for SDS-PAGE was determined by the Bradford Assay (Bio-Rad).

2.6 Western blotting

Western blot analysis was carried out by following a previous protocol [49]. Briefly, proteins on a SDS-PAGE gel were transferred to a PVDF membrane using semidry transfer apparatus (Bio-Rad). The membrane was blocked by

treating with Blocking One reagent (Nacalai Tesque Co. Ltd, Kyoto, Japan) over night at 4°C. This pretreated membrane was probed for testing immune-reactivity with anti-ribulose-1,5-bisphosphate carboxylase/oxygenase (RuBisCO) large subunit antibody (Catalog AS03 037-10, Agrisera, Vännäs, Sweden). This was followed by washing the membrane with TBS-Tween [50 mM Tris-HCl pH 8.2, 0.1% v/v Tween 20, 150 mM NaCl] for 5 min three times. Finally, the membrane was incubated in a 1:20 000 solution of alkaline phosphatase-conjugated anti-goat IgG (Bio-Rad) for 1 h at room temperature. Immunologically positive signals from protein bands were visualized using the CDP-star detection reagent and FUJIFILM ImageQuant LAS 4000 mini (GE Healthcare Bio-Sciences KK, Tokyo, Japan).

2.7 Protein database construction

We used the Trinity platform for constructing the *T. lutea* database by referring a previous study [50]. To complete protein database, we assembled transcriptomic data (SRR824147) [51] obtained from DDBJ (http://trace.ddbj.nig.ac.jp/DRASearch/) by using default Trinity [52] settings. Prior to assembly preprocessing of transcriptomic data was done with FASTX Toolkit (http://hannonlab.csh1.edu/fastx_toolkit/) to remove low quality ($Q < 20$) reads. Then, those assembled RNA sequences were converted to protein sequences using Bio-Perl.

2.8 Mass spectrometry analysis of proteins

LC-MS/MS analyses were conducted as described in our previous study [53]. Proteins of AB1, AB2 were analyzed, we also excised and analyzed five visible protein bands derived from AB1. Proteins were separated using a ready-made 12.5% w/v SDS-polyacrylamide gel (ATTO, Tokyo, Japan) and stained with Flamingo (Bio-Rad). Each lane with several protein bands was sliced into eight pieces of equal length and washed twice with HPLC-grade water containing 60% v/v acetonitrile (Kanto Chemical, Tokyo, Japan) and 50 mM ammonium bicarbonate. Then, the gel pieces were incubated in solution with 10 mM DTT and 50 mM ammonium bicarbonate for 45 min at 56°C, followed by another incubation in 55 mM iodoacetamide and 50 mM ammonium bicarbonate for 30 min at room temperature. The gels were washed twice with HPLC-grade water containing 60% v/v acetonitrile and 50 mM ammonium bicarbonate and dried in a vacuum concentrator. The dried gel pieces were incubated with 2 μL of a 10 ng/μL trypsin (MS grade gold; Promega, Wisconsin, USA) and 50 mM ammonium bicarbonate at 37°C for 16 h. After transferring digested peptides to a new microfuge tube, the gel was treated twice with 20 μL of 0.2% v/v formic acid (Wako, Tokyo, Japan) and 50% v/v acetonitrile, and then all extracted peptides were collected and combined in to a new microfuge tube. The extracts were dried in a vacuum concentrator and dissolved into a mixture of 0.1% v/v formic acid and 5% v/v acetonitrile. The dissolved solution was filtered by the Ultrafree-MC Centrifugal Filters (PVDF 0.45 μm; Millipore, Massachusetts, USA) to avoid contamination of gel pieces. LC-MS/MS analyses were performed using the LTQ-Orbitrap XL-HTC-PAL system (Thermo Fisher Scientific, Bremen, Germany). As a sample for analysis, the trypsin digests were loaded onto the column (100 μm internal diameter, 15-cm length; L-Column, CERI) using the Paradigm MS4 HPLC pump (Michrom BioResources, CA, USA) and HTC-PAL autosampler (CTC Analytics, Zwingen, Switzerland), and then eluted by a gradient of 5–45% v/v acetonitrile in 0.1% v/v formic acid for 26 min. The eluted peptides were introduced directly into an LTQ-Orbitrap with a flow rate of 500 nL/min and a spray voltage of 2.0 kV. MS/MS spectra were analyzed by MASCOT server (version 2.4) in house (http://www.matrixscience.com/) and the profiles were compared with those annotated from *T. lutea* transcriptome database according to a recent publication [51]. The MASCOT search parameters were as follows: set off the threshold at 0.05 in the ion-score cut off, peptide tolerance at 10 ppm, MS/MS tolerance at ±0.5 Da, peptide charge of 2^+ or 3^+, trypsin as enzyme allowing up to one missed cleavage, carbamidomethylation on cysteine as a fixed modification and oxidation on methionine as a variable modification. In addition, a BLAST (http://www.ncbi.nlm.nih.gov/) database was also used for further detailed analysis as described below.

2.9 BLAST annotation

We used Blast2GO (V 2.7.2) (http://www.blast2go.com/b2ghome) for annotation of peptide sequences [54]. As MASCOT search engine analyzes the MS-MS spectra, it identifies peptide fragments and assigns them to proteins of the constructed *T. leutia* database. We considered the transcript sequences of such identified proteins as complete peptide sequences of the related peptide fragments. These sequences of peptide fragments were submitted to the BLAST Blast2GO java web start for annotation. This software is connected to the BLAST database where similarity searches will be performed for the query sequences. Available annotations and GO terms from the obtained hits were statistically analyzed by Blast2GO and the probable annotations were assigned to the query sequences. The peptide FASTA file with 755 peptide sequences was given as input to Blast2GO. In this tool, we used "blastp" to search for hits in "nr" (nonredundant) database to identify at least 100 best alignments with a minimum *e*-value cutoff of $1.0\ e^{-3}$ and annotation parameters like GO-weight cutoff and Annotation threshold parameters were set to default (GO-weight = 5; Annotation threshold = 55). All query peptide sequences with BLAST hits were assigned with a description that is the most probable function of the detected hits. We also performed InterProScan available in the tool, to allow annotation based on their domain information. This was followed by mapping of functional information

using GO data of the identified BLAST hits. The process of assigning functional terms to query sequences from the pool of GO terms gathered in the mapping step is based on the gene ontology vocabulary. The algorithm computes annotation score basing on quality of GO assignments and evidence code. Finally, annotations were assigned for those sequences that qualify the threshold value. These annotations are presented in Supporting Information Table 1 along with their peptide MASCOT results. Further, we selected most abundant peptide sequences from each sample based on their MASCOT score if Mol% is more than 1%. Thus a total of 70 abundant peptides were reanalyzed for their annotations using Blast2GO with same settings. Peptide sequences without any Blast hits were left unannotated. The sequence data of 70 abundant sequences are shown in Supporting Information Table 2.

3 Results

3.1 Algal growth and microscopic observation of LBs

The change in LBs in intact cells was observed under fluorescent microscope when *T. lutea* cells were initiated to grow in N-sufficient medium (final concentration of nitrate: 1.4 mM) in a batch culture (Fig. 1). However, it was found that the nitrate concentration decreased and finally depleted after approximately 9 days at the early stationary phase in separate experiments (data not shown). LBs observed as BODIPY-stained neutral lipid particles in intact cells were very tiny at the logarithmic growth phase and became more obvious when growth stage proceeded close to the stationary growth phases after 10 days (Fig. 1).

When the stationary growth phase cells at day 17 were transferred to fresh –N medium, the size of LBs became larger and larger while chlorophyll fluorescence started to decay (Fig. 2, Supporting Information Fig. 1). In *T. lutea*, the LBs remain as individual entities without fusing with each other, but appear to be one large LB because of overlapped images under the microscope (Figs. 1 and 2). This feature is different from LBs of the unicellular green alga *Chlorella* in which large-sized lipid body was formed by fusion of several LBs in the cell [39]. LBs of *Chlorella* mainly contains TAG but biochemical analysis of the whole cellular lipids in *T. lutea* cells showed a high content of the alkenones [6–8]. Owing to the difference in the components of lipid molecules and proteins present in *T. lutea* LBs, such difference in LB formation may be observed.

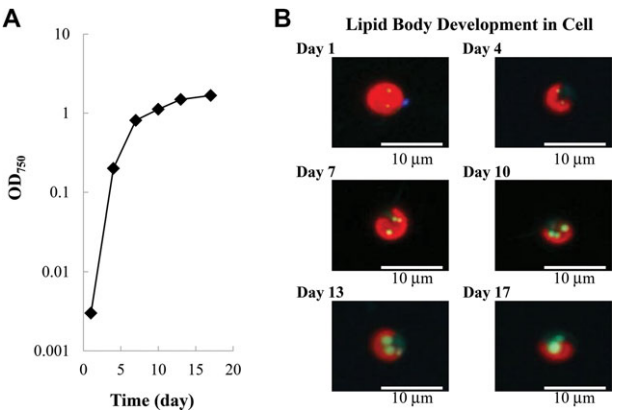

Figure 1. Cell growth curve and AB formation in the batch culture of haptophyte *T. lutea*. (A) Growth curve. (B) Representative pictures of ABs formation during cell growth. Cells were stained with BODIPY 493/503. Cells size, ca. 5 μm in diameter.

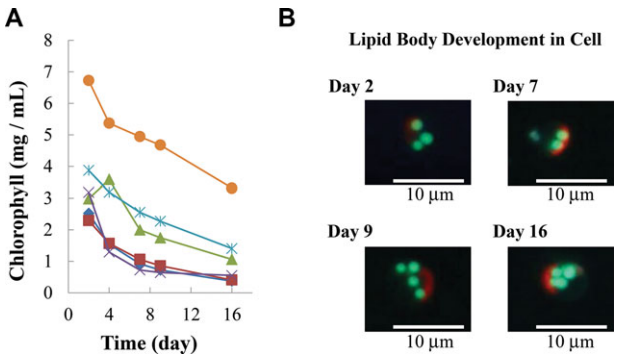

Figure 2. Changes in chlorophyll contents and fluorescent images of ABs after transferring 17-d culture cells into N-deficient medium. (A) Chlorophyll content in six experiments with different cell densities. Symbols indicate the same experimental cultures with different cell density separated into different bottles: bottle 1 (circle), bottle 2 (asterisk), bottle 3 (triangle), bottle 4 (cross), bottle 5 (diamond), and bottle 6 (square). (B) ABs stained by BODIPY 493/503 under fluorescence microscope. Cell size, ca. 5 μm in diameter.

3.2 Isolating LBs from *T. lutea*

In this study, we established a modified method for LB isolation from the haptophyte *T. lutea* (Fig. 3A). After the French Press treatment for breaking the cells, nuclear contamination was removed by a low speed centrifugation to obtain the PNS. In the PNS fraction a large number of round-shaped BODIPY-stained vesicles, namely isolated LBs, were observed, but some contamination of broken cell debris was also observed (Fig. 3B and C).

Next, the PNS fraction was applied to a sucrose density gradient centrifugation with six stepwise density-layers of sucrose (see Materials and methods). All visible debris and membranes of broken cells were separated into the respective layers. When the fraction of each layer was carefully observed under the microscope, most LBs were found floating in the fraction on top of the most upper layer (Fig. 4). As PNS suspended in 1 M sucrose was applied to 1 M sucrose layer (the second layer from the bottom in Fig. 4A), some debris

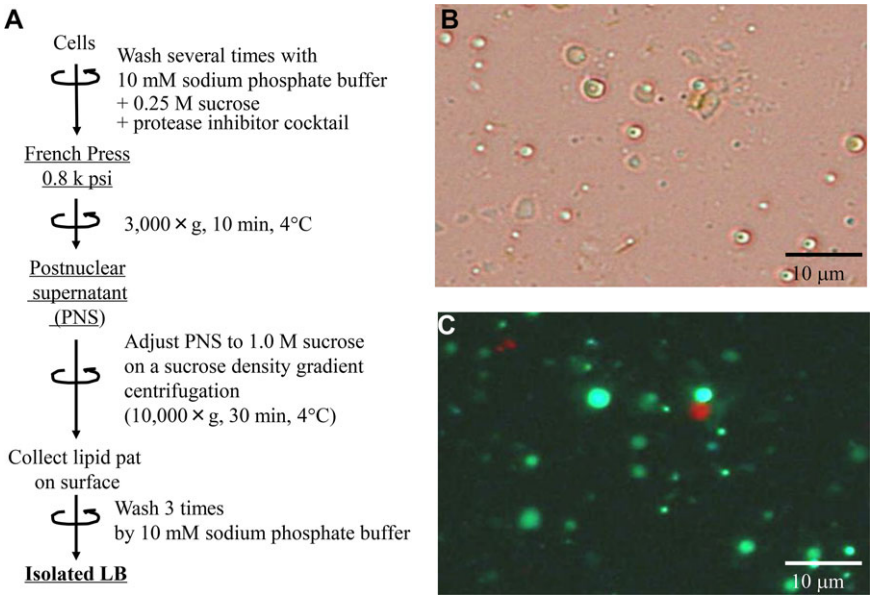

Figure 3. Newly established protocol for isolation of postnuclear supernatant (PNS) and ABs from N-deficient cells of haptophyte *T. lutea*. (A) Workflow of method for AB isolation. For sucrose gradient centrifugation, PNS in 1 M sucrose was placed in 1 M sucrose layer before centrifugation. (B) and (C): Bright view and fluorescent microscopic images of PNS stained with BODIPY 493/503. Green, ABs; red, chlorophyll auto-fluorescence.

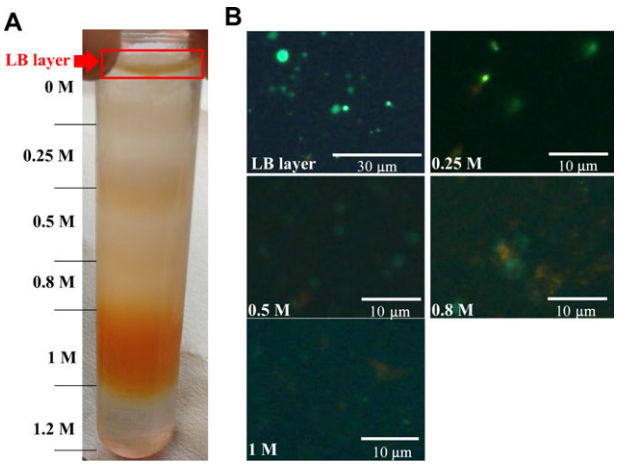

Figure 4. Purification of ABs by sucrose gradient centrifugation of PNS from N-deficient cells of haptophyte *T. lutea*. (A) Image of fractionation of ABs after stepwise sucrose density centrifugation. ABs were collected as a lipid pat on top. (B) Fluorescent microscopic images of granules stained with BODIPY 493/503. Green, ABs; red, chlorophyll auto-fluorescence.

attached to LBs could be removed during floating through several sucrose layers.

Microscopic images of BODIPY-stained purified LBs under both bright field and fluorescence microscopes showed no obvious contamination of chloroplasts in the obtained LB fraction (Fig. 5A and B). Repeatability of this method for isolating LBs was confirmed by microscopic observations in additional experiments (Supporting Information Fig. 2). These results show that the purified LBs isolated from *T. lutea* are composed of neutral lipids and commonly spherical in shape with a size ranging from 0.1 to 2 μm.

In this study, components of the purified LBs of *T. lutea* were firstly analyzed by GC-FID and three repeated analysis showed the presence of long-chain alkenones (mainly C_{37} and C_{38}) as major component (average content of total lipids: 74.2%), long-chain alkenes (1.2%), and others (24.6%) (Table 1, Supporting Information Fig. 3, Supporting Information Table 3). Fatty acids were negligible, meaning below the sensitivity of detection by both GC-FID and GC-MS, compared with the amount of LBs used for neutral lipids analysis. Based on these results, we inferred that LBs in Isochrysidales *T. lutea* (Haptophyte) can be called as the "alkenone body (hereafter, AB)." Thus ABs may serve as a storage center for neutral lipids in *T. lutea* cells since the present results are in accordance with the function of LBs described in a previous report on *I. galbana* and *E. huxleyi* [15]. The recovery rates of alkenones during the isolation and purification process of ABs from 40-L culture cells were 0.027–0.11% in two separate experiments. Isolation efficiency of ABs from whole cells was very low since the loss of ABs was quite high during the process of cell disruption.

3.3 SDS-PAGE and Western blot analysis of AB proteins in *T. lutea*

Properties of LBs, especially the contents of proteins and lipids in their amounts and categories, have been reported to vary among algal species [15, 25, 56]. It was also reported that the methods used for protein extraction affect protein amount in sugarcane [57]. As no generally applicable method is available for different organisms, we decided to develop a method by modification of previously reported methods that

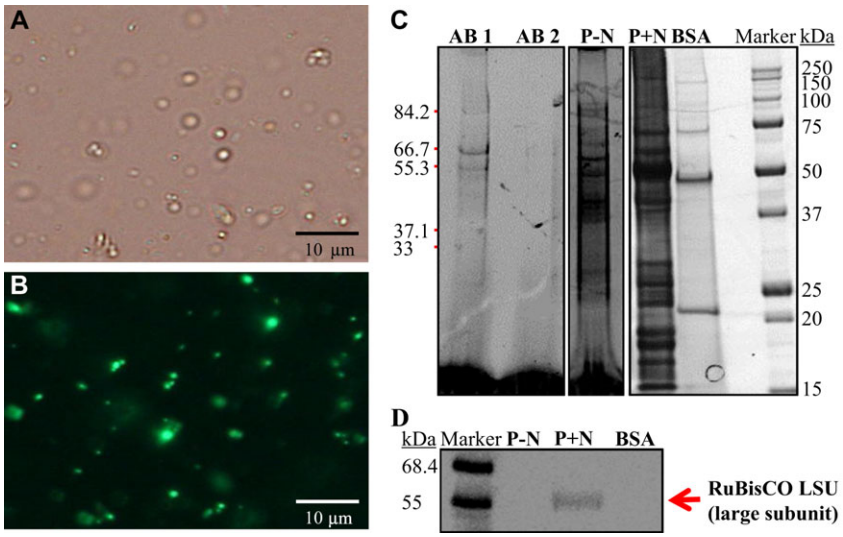

Figure 5. Microscopic images of purified ABs, profiles of proteins on SDS-PAGE and Western blot analysis of the purified ABs isolated from N-deficient cells of haptophyte *T. lutea*. (A) Bright view image. (B) Fluorescent microscopic image of ABs stained with BODIPY 493/503 showing no visible chlorophyll auto-fluorescence. (C) SDS-PAGE profile on 12.5% gel. Proteins applied: AB1 (3 μg), AB2 (2 μg), P-N (10 μg), P+N (10 μg) from *T. lutea*, and commercial BSA (10 μg) used as negative control. Marker: Molecular mass markers (with kDa). P-N and P+N: PNS from N-deficient cells (PNS/-N) and –sufficient cells (PNS/+N) as control, respectively. (D) Western blotting to reveal RuBisCO contamination or not in PNS/-N (P-N) and PNS/+N (P+N) from *T. lutea*, and BSA as control. Total proteins applied to each lane: 10 μg. Probe: antibody against RuBisCO large subunit.

Table 1. Composition of neutral lipids in purified LBs isolated from N-starved cells of haptophyte *T. lutea*

	Percentage (%) of total neutral lipids		
Sample no.	Alkenone (%)	Alkene (%)	Others (%)
LB-a	70.9	1.4	27.7
LB-b	74.2	1.0	24.8
LB-c	77.6	1.2	21.2
Average	74.2	1.2	24.6

Each fraction applied for GC-MS analysis was prepared by fractiontion with different organic solvents as described in Materials and methods. Experiments were repeated three times for whole process of algal growth, AB isolation/purification, lipid extraction, and GC analysis of lipids.

could be applicable for the extraction of LB proteins from alkenone-producing algae.

We compared two methods for extracting lipids from ABs of *T. lutea* in order to obtain proteins from purified LB and a well-resolved SDS-PAGE profile therein. Two organic solvents, namely 90% acetone and petroleum ether were used for preparing the AB1 and AB2 samples, respectively (Fig. 5C). Even on SDS-PAGE in which highest amount of proteins (ca. 3 and 2 μg for AB1 and AB2, respectively) was applied on each lane, AB1 produced clearer protein bands in comparison with AB2. This result suggests that acetone is better than petroleum ether as organic solvent for removing lipids and preparing pure proteins for use in downstream proteomic analysis.

In the control (PNS of N-sufficient cells, PNS/+N), Rubisco (55 kDa) was abundantly seen, whereas no such clear band was observed in the PNS of N-deficient cells (PNS/-N) (Fig. 5C). These results indicate that cells grown in N-deficient medium are suitable for isolating LB because of the low content of proteins that might serve as contaminants, and it is similar to a previously reported study on *Chlamydomonas* [35]. There also are difference in both high and low molecular mass of proteins between PNS/+N and PNS/-N. This may be due to down regulation of those proteins under long time nitrogen depletion [52].

Western blot analysis with anti-RuBisCO antibody showed that ABs purified from PNS/-N contained no contamination of this chloroplast-located major protein, indicating that LBs were purified (Fig. 5D). The purity of LBs was demonstrated by calculating proteins/alkenones ratio in PNS and isolated LBs fractions since alkenones are the main component of lipid bodies (therefore named as ABs) in *T. lutea* (see Table 1). The ratio of proteins/alkenones in ABs decreased to 1/5–1/7 times lower values in comparison with that in PNS (crude extracts) in two separate experiments.

Therefore, N-deficient cell culture approach works not only to increase neutral lipid contents and also to reduce chloroplastic proteins. Our present results confirmed the previous study reporting that better isolation quality of LBs was obtained in cells grown under N-deficient conditions than that from control [35].

3.4 Proteomics of ABs from *T. lutea*

The protein composition of two purified AB samples, namely AB1 and AB2, isolated from *T. lutea* was determined by LC-MS/MS analysis (see Materials and methods). Annotated lists of matched proteins were compiled and ranked by their relative abundance based on exponentially modified protein abundance index (emPAI). The parameter Mol%, calculated by the equation of $[(\text{emPAI})/\Sigma(\text{emPAI})] \times 100\%$, represents the protein abundance in each subcellular fraction [58, 59]. Identification of AB proteins of *T. lutea* was determined by searching the highest sequence similarity in the database using BLAST search. Peptide sequences obtained from the LC-MS/MS analysis were also compared to the *T. lutea* protein

Table 2. List of top 18 peptides identified by proteomics and database search (mol% ≥ 1%) in AB1 of the N-deficient cells of haptophyte *T. Lutea*

No.	Seq. name	Description	Mass	Score	Mol%	emPAI	Function
1	comp4668_c0_seq1	v-Type H^+ ATPase subunit E	26 110	729	10.1	33.4	Protons pump
2	comp4693_c0_seq1	Vacuolar H^+ ATPase A subunit	68 574	2758	6.2	20.3	Protons pump
3	comp19058_c0_seq1	Hypothetical protein EMIHUDRAFT_465517	44 412	2605	5.8	19.0	Unknown
4	comp16531_c0_seq1	v-Type proton ATPase subunit brain isoform	55 607	2638	5.7	18.8	Protons pump
5	comp16610_c0_seq1	Hypersensitive-induced response protein 1/SPFH domain containing protein	34 847	730	4.1	13.4	Unknown
6	comp16813_c0_seq1	Cycloartenol-c-24-methyltransferase 1-like	41 374	1413	3.1	10.3	Transferase
7	comp17799_c0_seq1	ATPase v_0 complex subunit d	42 020	588	1.9	6.1	Protons pump
8	comp17371_c0_seq1	Outer mitochondrial membrane protein porin	34 892	641	1.8	6.0	Unknown
9	comp4712_c1_seq3	Coccolith scale associated protein-1	74 258	1403	1.5	5.1	Unknown
10	comp4939_c0_seq1	Phosphate ABC transporter substrate-binding protein	99 738	2038	1.4	4.5	Unknown
11	comp14366_c0_seq2	actin	32 986	808	1.2	4.1	Cytoskeleton
12	comp4619_c0_seq1	FAD-dependent pyridine nucleotide-disulfide oxidoreductase	47 372	1069	1.2	3.9	Unknown
13	comp15167_c1_seq1	Actin	46 230	957	1.1	3.8	Cytoskeleton
14	comp16872_c0_seq1	ATP synthase subunit mitochondrial-like	55 639	1018	1.1	3.7	Energy metabolism
15	comp17302_c0_seq1	Short-chain dehydrogenase reductase sdr	39 518	926	1.1	3.7	Unknown
16	comp13695_c0_seq1	Light harvesting protein	8904	93	1.1	3.5	PSII
17	comp18572_c0_seq1	v-Type proton ATPase subunit h isoform x2	53 790	1120	1.0	3.4	Protons pump
18	comp18144_c0_seq1	Short-chain dehydrogenase reductase sdr	36 841	860	1.0	3.3	Unknown

For SDS-PAGE profile, see Fig. 5C.

database for finding proteins matched in identity (Supporting Information Tables 4–11).

In this proteomic analysis, we identified many proteins, but we mainly focus our discussion on the identified proteins with a Mol% over 1%. In AB1, 514 protein sequences were totally annotated (Supporting Information Table 4). Among them, top 18 hypothetically annotated proteins are listed in Table 2. Top 5 hypothetical functions annotated in AB1 (with number of reads in parenthesis) were proton pumps (V-ATPase) (5), cytoskeletons (2), transferases (1), energy metabolisms (1), and photosystem II (1) (shown diagramatically in Fig. 6A). Because of unclear image of AB2, we will focus on only AB1 to discuss the obtained proteomics data and use the AB2 data as a supporting data on the identification of major proteins in AB2 (Supporting Information Tables 5 and 6).

The proteins matched with the highest Mol% in AB1 is V-type H+-ATPase (V-ATPase). The Mol% values were 6.4, 5.7 10.1, and 1.9 in V1 sector subunit A, B, E, and V_0 sector subunit d, respectively (Table 2; For AB2, see Supporting Information Tables 5 and 6). The abundant proteins identified in ABs of *T. lutea* such as proton pump (V-ATPase) and energy metabolism (ATPase) may play some important role during the formation and development of ABs. The other abundant proteins comprised a hypothetical protein EMIHUDRAFT_465517 (5.8%), SPFH domain-containing protein (4.1%), coccolith scale associated protein-1 (1.5%), FAD-dependent pyridine nucleotide-disulfide oxidoreductase (1.2%), phosphate ABC transporter substrate-binding protein (1.4%), outer mitochondrial membrane protein of porin (1.8%), and cycloartenol-c-24-methyltransferase 1-like protein (3.1%) (Table 2). In addition, actin, short-chain dehydrogenase reductase (SDR) and ATP synthase were also detected. Despite many purification steps of our ABs, some proteins such as the light harvesting protein that is closely related to PSII were also identified. It suggests that there is still some tiny amount of contaminated proteins in our AB samples.

As visible protein bands were detected in the AB1 protein sample (Fig. 5C), we wanted to know what these proteins are and to reconfirm the major proteins present in ABs. Therefore, in an independent experiment, we excised and analyzed five specific bands cut out from SDS-PAGE gel to obtain more information on proteins over the slice analysis. The five major bands with molecular masses (kDa) of 84.2, 66.7, 55.3, 37.1, and 33.0 (AB1 in Fig. 5C) were separately brought to proteomic analysis.

According to the similarity search of sequenced peptides in database (Table 3, Supporting Information Tables 7–11), various subunits of V-ATPase were identified predominantly in three bands with molecular masses of 66.7, 55.3, and 33.0 kDa. Further, both a phosphate ABC transporter substrate-binding protein and a hypothetical protein EMIHUDRAFT_465517 were dominantly identified in the 84.2 kDa band. In the 37.1 kDa band, a cyclocartenol-*c*-24-methyltransferase 1-like protein, expected to be an enzyme belonging to a family of sterol 24-C-methyltransferases that perform distinctive activity to transfer C_1-residue, was identified as the dominant protein (Table 3). Functional category can be seen in Fig. 6B.

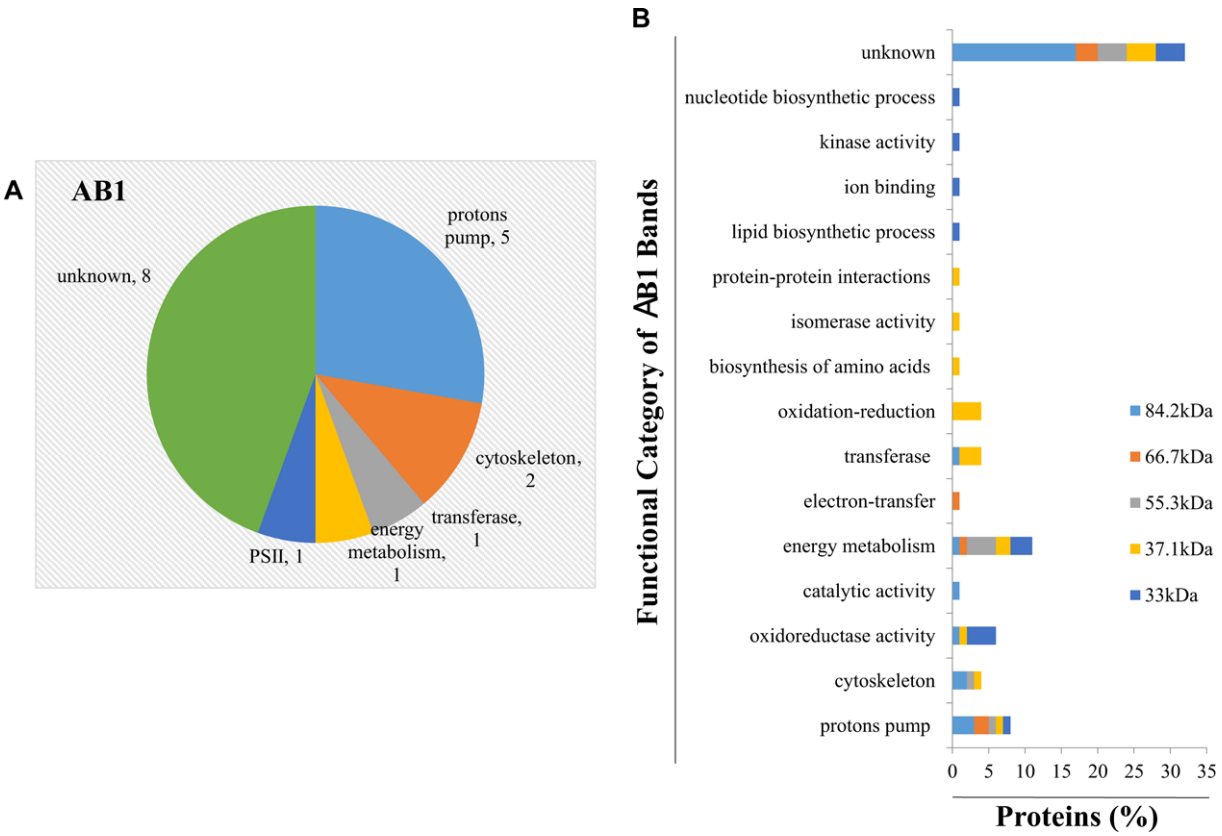

Figure 6. Category of hypothetical functions of abundant proteins in ABs from N-deficient cells of haptophyte *T. lutea*. (A) AB1. (B) Categories of hypothetical functions of proteins identified from the five abundant protein bands on SDS-PAGE of AB1.

4 Discussion

4.1 Isolation of ABs from *T. lutea*

The cell structure of the secondary symbiotic algal species such as *T. lutea* is generally known to be very different from the primary symbiotic algae. It has four layers of chloroplast envelopes with an ER membrane at the outmost position. Therefore, isolation of LBs would be more difficult in the secondary symbiotic algae such as haptophytes in comparison with the primary symbiotic algae such as green algae and higher plants.

The isolation of LBs was previously reported in the haptophyte *I. galbana* CCMP 1323, unicellular green microalgae such as *Chlamydomonas* and *Chlorella* in microalgae and in plants as well [15, 36, 39, 46, 60]. By replicating methods described in the previous reports, we attempted to isolate the ABs from *T. lutea* several times, but were not successful in obtaining better quality ABs, primarily because of chloroplast contamination. Such failure may be due to different lipid contents, different cell properties or morphology of LBs in each species. Even though *T. lutea* is a sister taxon of *I. galbana*, some differences in their lipid contents and profiles as well are expected. We list the previous methods for LB isolation from various organisms and also describe some possible reasons of our failure in our experiments with *T. lutea* for further argument although the exact reasons are not fully known (Supporting Information Table 12).

We recognize three important points for the successful isolation and purification of ABs of *T. lutea* in this study. The first point relates to the preparation of very large AB-harboring cells that were obtained by maintaining cells under –N conditions for 16 days (Fig. 2). This condition was used since LBs are generally known to be enlarged under –N conditions in other taxonomically different microalgae [60–62] as well as in haptophytes *I. galbana* and *T. lutea* [15, 52]. Additionally, N-deficient culture was also effective in decreasing RuBisCO contamination in AB fraction since chloroplasts were degraded during incubation as confirmed by the absence of chlorophyll auto-fluorescence under fluorescent microscope (red fluorescence in Fig. 2, Supporting Information Fig. 1).

The second important strategy for isolation ABs was an improvement of the cell disruption method. Initially, we tested many kinds of cell disruption methods, such as the Yeda press connected to a compressed nitrogen gas cylinder, sonication, grinding by motor, and pestle under liquid nitrogen and a French Press. Finally, we found that the French Press

Table 3. Identification of top 5 major bands on SDS-PAGE of AB1 of the N-deficient cells of haptophyte *T. lutea* by proteomis and database search (mol% ≥ 1%)

No.	Seq. name	Description	Mass	Score	Mol%	emPAI	Function
84.2 kDa							
1	comp4939_c0_seq1	Phosphate ABC transporter substrate-binding protein	99 738	1509	17.9	4.0	Unknown
2	comp19058_c0_seq1	Hypothetical protein EMIHUDRAFT_465517	44 412	467	13.4	3.0	Unknown
3	comp26472_c0_seq1	—NA—	56 244	291	4.1	0.9	Unknown
4	comp1465224_c0_seq1	—NA—	—	18	4.1	0.9	Unknown
5	comp4693_c0_seq1	Vacuolar H^+ ATPase a subunit	68 574	355	3.6	0.8	Protons pump
66.7 kDa							
1	comp4693_c0_seq1	Vacuolar H^+ ATPase a subunit	68 574	2701	62.9	35.1	Protons pump
2	comp4712_c1_seq3	Coccolith scale associated protein-1	74 258	1713	11.5	6.4	unknown
3	comp19058_c0_seq1	Hypothetical protein EMIHUDRAFT_465517	44 412	185	1.9	1.1	Unknown
4	comp13701_c0_seq1	Succinate dehydrogenase	65 131	312	1.7	1.0	Energy metabolism
5	comp1465224_c0_seq1	—NA—	—	17	1.6	0.9	Unknown
55.3 kDa							
1	comp16531_c0_seq1	v-Type proton ATPase subunit brain isoform	55 607	2386	53.1	42.0	Protons pump
2	comp16872_c0_seq1	ATP synthase subunit mitochondrial-like	55 639	1117	11.0	8.7	Energy metabolism
3	comp16982_c0_seq1	ATP synthase F1 subunit alpha	59 044	1261	7.7	6.1	Energy metabolism
4	comp14581_c0_seq2	ATP synthase cf1 alpha subunit	54 333	481	2.6	2.1	Energy metabolism
5	comp19058_c0_seq1	Hypothetical protein EMIHUDRAFT_465517	44 412	365	1.8	1.4	Unknown
37.1 kDa							
1	comp16813_c0_seq1	Cycloartenol-c-24-methyltransferase 1-like	41 374	732	32.6	15.0	Transferase
2	comp20854_c0_seq1	Saccharopine dehydrogenase	46 327	533	6.6	3.1	Oxidoreductase activity
3	comp52449_c0_seq1	Glutathione s-transferase	41 399	526	5.8	2.7	Transferase
4	comp20217_c0_seq1	Cysteine synthase	41 103	353	5.2	2.4	Transferase
5	comp18144_c0_seq1	Short-chain dehydrogenase reductase sdr	36 841	286	4.1	1.9	Oxidation-reduction
33 kDa							
1	comp17799_c0_seq1	Vacuolar ATPase subunit DVA41	42 020	760	14.8	5.5	Protons pump
2	comp17302_c0_seq1	Short-chain dehydrogenase reductase sdr	39 518	469	11.0	4.1	Oxidoreductase activity
3	comp21189_c0_seq1	Prohibitin	38 082	320	9.4	3.5	
4	comp18144_c0_seq1	Short-chain dehydrogenase reductase sdr	36 841	409	7.8	2.9	Oxidoreductase activity
5	comp16610_c0_seq1	SPFH domain-containing protein	34 847	205	5.6	2.1	Unknown

For SDS-PAGE profile, see Fig. 5C.

was the best method for *T. lutea* cell disruption based on the efficiency of recovery and purity of ABs isolated. In this method, the high amount of ABs was easily obtained as a lipid body pat on top of the layer following sucrose density gradient centrifugation (Fig. 4).

The third point is related to the sucrose gradient step, and involved using six different sucrose density layers in our experiment in order to enhance the washing effect and remove all visible debris and membranes derived from broken cells. Therefore, ABs were effectively separated as the "alkenone body layer" floating onto the top of the centrifuge tube and purified by removal of attached materials on AB surface during passing through several sucrose layers (Fig. 4A).

4.2 AB proteins of *T. lutea*

There are different types of LBs in plant seeds and leaves [63]. V-type H^+-ATPase was detected as major component of LBs in leaves of TAG-producing higher plants such as *Arabidopsis* [30] and mesocarp tissue of avocado [60]. However, the protein V-ATPase has not been found in seed LBs until now. Interestingly, V-ATPase has been identified from *T. lutea* cells cultured under N-deficient conditions [64]. The V_1 subunit of V-ATPase is known to be responsible for ATP hydrolysis whereas V_0 subunit for transporting H^+ across the membrane [65]. Although, V-ATPase is localized in the tonoplast (vacuolar membrane), Golgi apparatus and in other coated vesicles in eukaryotes, the subunit V_0 is typically localized in the ER membrane where the whole molecule of V-ATPase is assembled [20, 65–69]. It was reported that the haptophyte *E. huxleyi*, a sister taxon of *T. lutea*, produces alkenones by associating with internal organelles such as the ER and the coccolith-producing compartment [20]. The coccolith-producing compartment is thought to contain V-ATPase exporting protons for calcification, and is known to be formed by budding from the Golgi body whose membrane is closely associated with ER [70, 71]. According to the ultrastructure analysis of LB formation in *T. lutea*, LBs were always observed to appear by attaching closely to the outer

membrane of ER [7]. It was also reported that a g6574 protein identified by proteomics study of LB in the oleaginous diatom *Fistulifera solaris* exist in both ER and LBs [61]. As the secondary symbiotic microalga, this diatom also has a four-layered chloroplast envelope, of which the outmost plastid envelope is connected to the outer membrane of ER.

Based on all these known evidence, it seems that the V-ATPase is most likely assembled in ER as the major protein of ABs in *T. lutea*. Therefore, we hypothesize that neutral lipids involving alkenones as the major component are first accumulated in the internal space of ER membranes through the support of V-ATPase located on the outer membrane of ER. Following the accumulation of neutral lipids in the vicinity, the budding of ABs from ER might be promoted, as modeled in Supporting Information Fig. 4. As ABs observed in the logarithmic growth phase were very small and which enlarged during the cell growth stage (Fig. 1), alkenones are also needed to be transported through the AB membrane.

Homologous protein of the hypothetical protein EMIHUDRAFT_465517 was found only in haptophytes by BLAST search in National Center for Biotechnology Information. Moreover, those sequences were quite similar among alkenone producers which are limited only to the haptophytes in BLAST homolog search by using protein database in Marine Microbial Eukaryote Transcriptome Sequencing Project (http://camera.calit2.net/mmetsp/combinedassemblies.php) (Supporting Information Table 13). It is tempting to suggest that the hypothetical protein EMIHUDRAFT_465517 is related to alkenone production or metabolism (For amino sequence, see Supporting Information Table 2).

The SPFH domain-containing protein was previously found in the plasma membrane, Golgi apparatus, lipid droplets, mitochondria, and ER [72–74]. It has been suggested that this protein is possibly involved in lipid raft and membrane microdomains [75], but the molecular basis of its function remains unknown. The SPFH domain-containing protein located in the ER membrane may be involved in LBs, especially during the process of budding of LBs, as suggested in Supporting Information Fig. 4.

In our study, a coccolith scale associated protein-1 was also identified as one of the AB-associated proteins in alkenone-producing but noncoccolith-producing haptophytes (Tables 2 and 3). This result is supported by the evidence that alkenones are localized in the coccolith-producing compartment in the coccolithophore *E. huxleyi* [20] and by a previous study that observed the increase in the relative abundance of the protein over six times under N-depletion conditions [52]. Interestingly, in the diatom *Phaeodactylum tricornutum*, this protein (AB537972.1 from the TAG-producing but nonalkenone-producing coccolithophore *Pleurochrysis carterae*) was also found as the most upregulated protein under N-depletion [76]. Although function of this protein in *T. lutea* remains unknown, its identification from the ABs indicates a contribution toward LB or AB formation in the secondary symbiotic marine microalgae.

We also identified a mitochondrial ATP synthase with low Mol% (1.1%) and emPAI (3.7) values, which was likely involved in energy metabolism pathways in accordance with results in a land plant *Arabidopsis* [30] and a marine coral-dinoflagellate endosymbiotic microalga [77]. A cycloartenol-*c*-24-methyltransferase 1-like protein was also identified, and this enzyme is known to be associated with steroid biosynthesis in higher plants such as soybean [78]. A novel AB protein short-chain dehydrogenase reductase SDR detected previously in *Brassica napus* [46] was suggested to have a possibly unknown function in LB structure, synthesis or degradation. In microalgae, the presence of brassicasterol and epigrassicasterol was confirmed in chromophyte algae such as diatoms and haptophytes including *Tisochrysis lutea* [79]. The enzyme *S*-adenosyl-L-methionine–cycloartenol methyltransferase activity was determined in green microalgae such as *Trebouxia* sp. and *Scenedesmus obliquus* [80]. However, the connection of this protein to alkenone metabolism remains to be clarified. The coexistence of these metabolites and proteins likely suggests that ABs represent not only just a lipid storage vesicle but also a location for lipid metabolism.

Actin protein identified in our study was determined to have cytoskeleton function. This protein has been detected previously in LB proteins of many species [30, 60, 63, 77]. Though it was thought to be specific to LBs [77], it is still unclear whether it has a function in LBs or appears as a contaminant. Histone protein has been previously suggested to be associated with LBs before transfer to nuclei during development [23, 77].

We also detected some minor proteins which may be involved in lipid metabolism in *T. lutea* (Supporting Information Table 4). Those proteins were long chain acyl-CoA synthetase that binds fatty acid to produce fatty acyl-CoA, cyclopropane-fatty-acyl-phospholipid synthase, malate dehydrogenase, and glycerol-3-phosphate dehydrogenase. These proteins were also reported in *Chlamydomonas* [36] along with additional proteins that are involved in acyl-lipid metabolism. This difference may be due to divergence in the species.

Finally, we would like to discuss on the uniqueness of the AB proteome based on our current knowledge of the proteins cataloged in this study. Unlike in higher plants [31–33], *C. reinhardtii* [35, 36] and other microalgae [37–40], we did not find oleosin, MLDP, HOSP, or LDSP in ABs of *T. lutea* (Tables 2 and 3). This result may be due to their phylogenetic differences [81, 82]. Therefore, it can be assumed that the V-ATPase in ABs may also function as structural protein that is similar to oleosin or MLDP in the LB since V-ATPase was largely contained as the major protein of ABs in *T. lutea*. To prove this hypothesis, generating antibodies against the V-ATPase subunit A and the hypothetical protein EMIHUDRAFT 465517 will be very useful to confirm the localization of these two proteins by immune-electron microscopy. Furthermore, it will be important to examine the expression of the genes encoding for these abundant proteins in order to reveal their possible metabolic pathways, in future studies.

4.3 Conclusions

Our present study in the alkenone-producing haptophyte *T. lutea* fulfilled the two main objectives, (i) establishment of a method to isolate ABs, and (ii) providing a significant lipid content and proteome dataset of the ABs. Proteomic analyses revealed V-ATPase as a major protein in ABs of *T. lutea*, and the inventory of identified proteins suggested that the ABs might be derived from the ER. Furthermore, we speculate that the abundant hypothetical protein EMIHUDRAFT 465517 might be strongly related with alkenone metabolism since the ABs dominantly contains alkenones. Future studies investigating these claims will provide valuable information for elucidating the mechanism of alkenone production in haptophytes. In addition, a deeper investigation will be required to reveal the whole process of LB formation in *T. lutea*.

This work was fully supported by CREST of the Japan Science and Technology Agency (JST) [CREST/JST] to Y.S. (FY2010-2015) and partly by Gant-in-Aid for Scientific Research for a Plant Graduate Student of the Nara Institute of Science and Technology (NAIST), Japan, to Q.S. We are grateful to proteome analysis team of NAIST for their kind assistance. Thanks are also given to Dr. Yufan Liu and Mr. Juan Miguel Recto for their kind helps in preparing this paper.

All authors declare no financial/commercial conflicts of interest.

5 References

[1] Liu, H., Probert, I., Uitz, J., Claustre, H. et al., Extreme diversity in noncalcifying haptophytes explains a major pigment paradox in open oceans. *Proc. Natl. Acad. Sci. USA* 2009, *106*, 12803–12808.

[2] Holligan, P. M., Viollier, M., Harbour, D. S., Camus, P. et al., Satellite and ship studies of coccolithophore production along a continental-shelf edge. *Nature* 1983, *304*, 339–342.

[3] Bendif, E., Probert, I., Schroeder, D. C., deVargas, C., On the description of *Tisochrysis lutea* gen. nov sp nov and *Isochrysis nuda* sp nov in the Isochrysidales, and the transfer of *Dicrateria* to the Prymnesiales (Haptophyta). *J. Appl. Phycol.* 2013, *25*, 1763–1776.

[4] Marchetti, J., Bougaran, G., LeDean, L., Megrier, C. et al., Optimizing conditions for the continuous culture of *Isochrysis* affinis *galbana* relevant to commercial hatcheries. *Aquaculture* 2012, *326*, 106–115.

[5] Alkhamis, Y., Qin, J. G., Cultivation of *Isochrysis galbana* in phototrophic, heterotrophic, and mixotrophic conditions. *Biomed. Res. Int.* 2013, *2013*, 1–9.

[6] Brown, M. R., Dunstan, G. A., Jeffrey, S. W., Volkman, J. K. et al., The influence of irradiance on the biochemical-composition of the prymnesiophyte *Isochrysis*sp (Clone T-Iso). *J. Phycol.* 1993, *29*, 601–612.

[7] Liu, C. P., Lin, L. P., Ultrastructural study and lipid formation of *Isochrysis* sp CCMP1324. *Bot. Bull. Acad. Sinica* 2001, *42*, 207–214.

[8] Sukenik, A., Wahnon, R., Biochemical quality of marine unicellular algae with special emphasis on lipid composition. *I. Isochrysis galbana. Aquaculture* 1991, *97*, 61–72.

[9] Marlowe, I. T., Brassell, S. C., Eglinton, G., Green, J. C., Long chain unsaturated ketones and esters in living algae and marine sediments. *Organic Geochem.* 1984, *6*, 135–141.

[10] Marlowe, I. T., Green, J. C., Neal, A. C., Brassell, S. C. et al., Long chain (*n*-C37-C39) alkenones in the *Prymnesiophyceae*. Distribution of alkenones and other lipids and their taxonomic significance. *Brit. Phycol. J.* 1984, *19*, 203–216.

[11] Rechka, J. A., Maxwell, J. R., Characterization of alkenone temperature indicators in sediments and organisms. *Organic Geochem.* 1988, *13*, 727–734.

[12] Theroux, S., D'Andrea, W.J., Toney, J., Amaral-Zettler, L., Huang, Y. S., Phylogenetic diversity and evolutionary relatedness of alkenone-producing haptophyte algae in lakes: Implications for continental paleotemperature reconstructions. *Earth Planet Sc. Lett.* 2010, *300*, 311–320.

[13] Prahl, F. G., Wakeham, S. G., Calibration of unsaturation patterns in long-chain ketone compositions for paleotemperature sssessment. *Nature* 1987, *330*, 367–369.

[14] Prahl, F., Herbert, T., Brassell, S. C., Ohkouchi, N. et al., Status of alkenone paleothermometer calibration: Report from Working Group 3. *Geochem. Geophy. Geosy.* 2000, *1*, 000–000.

[15] Eltgroth, M. L., Watwood, R. L., Wolfe, G. V., Production and cellular localization of neutral long-chain lipids in the haptophyte algae *Isochrysis galbana* and *Emiliania huxleyi*. *J. Phycol.* 2005, *41*, 1000–1009.

[16] Rodolfi, L., Zittelli, G. C., Bassi, N., Padovani, G. et al., Microalgae for oil: Strain selection, induction of lipid synthesis and outdoor mass cultivation in a low-cost photobioreactor. *Biotechnol. Bioeng.* 2009, *102*, 100–112.

[17] O'Neil, G. W., Knothe, G., Williams, J. R., Burlow, N. P. et al., Synthesis and analysis of an alkenone-free biodiesel from *Isochrysis* sp. *Energ. Fuel* 2014, *28*, 2677–2683.

[18] Bell, M. V., Pond, D., Lipid composition during growth of motile and coccolith forms of *Emiliania huxleyi*. *Phytochemistry* 1996, *41*, 465–471.

[19] Epstein, B. L., D'Hondt, S., Hargraves, P. E., The possible metabolic role of C-37 alkenones in *Emiliania huxleyi*. *Organic Geochem.* 2001, *32*, 867–875.

[20] Sawada, K., Shiraiwa, Y., Alkenone and alkenoic acid compositions of the membrane fractions of *Emiliania huxleyi*. *Phytochemistry* 2004, *65*, 1299–1307.

[21] Farese, R. V., Walther, T. C., Lipid droplets finally get a little R-E-S-P-E-C-T. *Cell* 2009, *139*, 855–860.

[22] Krahmer, N., Guo, Y., Farese, R. V., Walther, T. C., SnapShot: Lipid droplets. *Cell* 2009, *139*, 1024–U1192.

[23] Cermelli, S., Guo, Y., Gross, S. P., Welte, M. A., The lipid-droplet proteome reveals that droplets are a protein-storage depot. *Curr. Biol.* 2006, *16*, 1783–1795.

[24] Goodman, J. M., The gregarious lipid droplet. *J. Biol. Chem.* 2008, *283*, 28005–28009.

[25] Murphy, S., Martin, S., Parton, R. G., Lipid droplet-organelle interactions; sharing the fats. *Bba-Mol. Cell Biol. L* 2009, *1791*, 441–447.

[26] Zehmer, J. K., Huang, Y. G., Peng, G., Pu, J. et al., A role for lipid droplets in inter-membrane lipid traffic. *Proteomics* 2009, *9*, 914–921.

[27] Chapman, K. D., Dyer, J. M., Mullen, R. T., Biogenesis and functions of lipid droplets in plants. *J. Lipid Res.* 2012, *53*, 215–226.

[28] Li, Z. H., Thiel, K., Thul, P. J., Beller, M. et al., Lipid droplets control the maternal histone supply of *Drosophila* embryos. *Curr. Biol.* 2012, *22*, 2104–2113.

[29] Zechner, R., Zimmermann, R., Eichmann, T. O., Kohlwein, S. D. et al., FAT SIGNALS-Lipases and lipolysis in lipid metabolism and signaling. *Cell Metab.* 2012, *15*, 279–291.

[30] Shimada, T. L., Takano, Y., Shimada, T., Fujiwara, M. et al., Leaf oil body functions as a subcellular factory for the production of a phytoalexin in Arabidopsis. *Plant Physiol.* 2014, *164*, 105–118.

[31] Naested, H., Frandsen, G. I., Jauh, G. Y., Hernandez-Pinzon, I. et al., Caleosins: Ca^{2+}-binding proteins associated with lipid bodies. *Plant Mol. Biol.* 2000, *44*, 463–476.

[32] Lin, L. J., Tai, S. S. K., Peng, C. C., Tzen, J. T. C., Steroleosin, a sterol-binding dehydrogenase in seed oil bodies. *Plant Physiol.* 2002, *128*, 1200–1211.

[33] Siloto, R. M. P., Findlay, K., Lopez-Villalobos, A., Yeung, E. C. et al., The accumulation of oleosins determines the size of seed oilbodies in Arabidopsis. *Plant Cell* 2006, *18*, 1961–1974.

[34] d'Andréa, S., Canonge, M., Beopoulos, A., Jolivet, P. et al., At5g50600 encodes a member of the short-chain dehydrogenase reductase superfamily with 11β- and 17β-hydroxy steroid dehydrogenase activities associated with *Arabidopsis thaliana* seed oil bodies. *Biochimie* 2007, *89*, 222–229.

[35] Moellering, E. R., Benning, C., RNA interference silencing of a Major Lipid Droplet Protein affects lipid droplet size in *Chlamydomonas reinhardtii*. *Eukaryot. Cell* 2010, *9*, 97–106.

[36] Nguyen, H. M., Baudet, M., Cuine, S., Adriano, J. M. et al., Proteomic profiling of oil bodies isolated from the unicellular green microalga *Chlamydomonas reinhardtii*: with focus on proteins involved in lipid metabolism. *Proteomics* 2011, *11*, 4266–4273.

[37] Davidi, L., Katz, A., Pick, U., Characterization of major lipid droplet proteins from Dunaliella. *Planta* 2012, *236*, 19–33.

[38] Peled, E., Leu, S., Zarka, A., Weiss, M. et al., Isolation of a novel oil globule protein from the green alga *Haematococcus pluvialis* (Chlorophyceae). *Lipids* 2011, *46*, 851–861.

[39] Lin, I. P., Jiang, P. L., Chen, C. S., Tzen, J. T. C., A unique caleosin serving as the major integral protein in oil bodies isolated from *Chlorella* sp cells cultured with limited nitrogen. *Plant Physiol. Biochem.* 2012, *61*, 80–87.

[40] Vieler, A., Brubaker, S. B., Vick, B., Benning, C., A lipid droplet protein of *Nannochloropsis* with functions partially analogous to plant oleosins. *Plant Physiol.* 2012, *158*, 1562–1569.

[41] Heldt, H.-W., Piechulla, B., *Plant Biochemistry*, Elsevier Academic Press, The Netherlands 2011.

[42] Goodson, C., Roth, R., Wang, Z. T., Goodenough, U., Structural correlates of cytoplasmic and chloroplast lipid body synthesis in *Chlamydomonas reinhardtii* and stimulation of lipid body production with acetate boost. *Eukaryot. Cell.* 2011, *10*, 1592–1606.

[43] Bougaran, G., Rouxel, C., Dubois, N., Kaas, R. et al., Enhancement of neutral lipid productivity in the microalga *Isochrysis* affinis *Galbana* (T-Iso) by a mutation-selection procedure. *Biotechnol. Bioeng.* 2012, *109*, 2737–2745.

[44] Danbara, A., Shiraiwa, Y., The requirement of selenium for the growth of marine coccolithophorids, *Emiliania huxleyi*, *Gephyrocapsa oceanica* and *Helladosphaera* sp (Prymnesiophyceae). *Plant Cell Physiol.* 1999, *40*, 762–766.

[45] Ding, Y. F., Zhang, S. Y., Yang, L., Na, H. M. et al., Isolating lipid droplets from multiple species. *Nat. Protoc.* 2013, *8*, 43–51.

[46] Katavic, V., Agrawal, G. K., Hajduch, M., Harris, S. L., Thelen, J. J., Protein and lipid composition analysis of oil bodies from two *Brassica napus* cultivars. *Proteomics* 2006, *6*, 4586–4598.

[47] Kotajima, T., Shiraiwa, Y., Suzuki, I., Functional screening of a novel Δ15 fatty acid desaturase from the coccolithophorid *Emiliania huxleyi*. *BBA-Mol. Cell Biol. L* 2014, *1841*, 1451–1458.

[48] Agrawal, G., Jwa, N.-S., Jung, Y.-H., Kim, S. et al., in: Yang, Y. (Ed.), *Rice Protocols*, Humana Press, New York 2013, pp. 151–184.

[49] Tsuji, Y., Suzuki, I., Shiraiwa, Y., Enzymological evidence for the function of a plastid-located pyruvate carboxylase in the Haptophyte alga *Emiliania huxleyi*: a novel pathway for the production of C_4 Compounds. *Plant Cell Physiol.* 2012, *53*, 1043–1052.

[50] Haas, B. J., Papanicolaou, A., Yassour, M., Grabherr, M. et al., De novo transcript sequence reconstruction from RNA-seq using the trinity platform for reference generation and analysis. *Nat. Protoc.* 2013, *8*, 1494–1512.

[51] Carrier, G., Garnier, M., LeCunff, L., Bougaran, G. et al., Comparative transcriptome of wild type and selected strains of the microalgae *Tisochrysis lutea* provides insights into the genetic basis, lipid metabolism and the life cycle. *PLoS One* 2014, *9*, e86889.

[52] Garnier, M., Carrier, G., Rogniaux, H., Nicolau, E. et al., Comparative proteomics reveals proteins impacted by nitrogen deprivation in wild-type and high lipid-accumulating mutant strains of *Tisochrysis lutea*. *J. Proteomics* 2014, *105*, 107–120.

[53] Fujiwara, M., Uemura, T., Ebine, K., Nishimori, Y. et al., Interactomics of Qa-SNARE in *Arabidopsis thaliana*. *Plant Cell Physiol.* 2014, *55*, 781–789.

[54] Gotz, S., Garcia-Gomez, J. M., Terol, J., Williams, T. D. et al., High-throughput functional annotation and data mining with the Blast2GO suite. *Nucleic Acids Res.* 2008, *36*, 3420–3435.

[55] Conesa, A., Götz, S., Blast2GO: a comprehensive suite for functional analysis in plant genomics. *Int. J. Plant Genomics* 2008, *2008*, 12.

[56] Wang, Z. T., Ullrich, N., Joo, S., Waffenschmidt, S., Goodenough, U., Algal lipid bodies: stress induction, purification, and biochemical characterization in wild-type and starchless *Chlamydomonas reinhardtii*. *Eukaryot. Cell.* 2009, *8*, 1856–1868.

[57] Amalraj, R. S., Selvaraj, N., Veluswamy, G. K., Ramanujan, R. P. et al., Sugarcane proteomics: establishment of a protein extraction method for 2-DE in stalk tissues and initiation of sugarcane proteome reference map. *Electrophoresis* 2010, *31*, 1959–1974.

[58] Ishihama, Y., Oda, Y., Tabata, T., Sato, T. et al., Exponentially modified protein abundance index (emPAI) for estimation of absolute protein amount in proteomics by the number of sequenced peptides per protein. *Mol. Cell. Proteomics* 2005, *4*, 1265–1272.

[59] Baba, M., Suzuki, I., Shiraiwa, Y., Proteomic analysis of high-CO_2-inducible extracellular proteins in the unicellular green alga, *Chlamydomonas reinhardtii*. *Plant Cell Physiol.* 2011, *52*, 1302–1314.

[60] Horn, P. J., James, C. N., Gidda, S. K., Kilaru, A. et al., Identification of a new class of lipid droplet-associated proteins in plants. *Plant Physiol.* 2013, *162*, 1926–1936.

[61] Nojima, D., Yoshino, T., Maeda, Y., Tanaka, M. et al., Proteomics analysis of oil body-associated proteins in the oleaginous diatom. *J. Proteome Res.* 2013, *12*, 5293–5301.

[62] Pribyl, P., Cepak, V., Zachleder, V., Production of lipids and formation and mobilization of lipid bodies in *Chlorella vulgaris*. *J. Appl. Phycol.* 2013, *25*, 545–553.

[63] Jolivet, P., Acevedo, F., Boulard, C., d'Andrea, S. et al., Crop seed oil bodies: from challenges in protein identification to an emerging picture of the oil body proteome. *Proteomics* 2013, *13*, 1836–1849.

[64] Song, P. P., Li, L., Liu, J. G., Proteomic analysis in nitrogen-deprived *Isochrysis galbana* during lipid accumulation. *PLoS One* 2013, *8*, e82188.

[65] Marshansky, V., Futai, M., The V-type H^+-ATPase in vesicular trafficking: targeting, regulation and function. *Curr. Opin. Cell Biol.* 2008, *20*, 415–426.

[66] Bauerle, C., Ho, M. N., Lindorfer, M. A., Stevens, T. H., The *Saccharomyces cerevisiae VMA*6 gene encodes the 36-kDa subunit of the vacuolar H^+-ATPase membrane sector. *J. Biol. Chem.* 1993, *268*, 12749–12757.

[67] Kane, P. M., Tarsio, M., Liu, J. Z., Early steps in assembly of the yeast vacuolar H^+-ATPase. *J. Biol. Chem.* 1999, *274*, 17275–17283.

[68] Lee, S. K., Li, W., Ryu, S. E., Rhim, T., Ahnn, J., Vacuolar (H^+)-ATPases in *Caenorhabditis elegans*: what can we learn about giant H^+ pumps from tiny worms? *Bba-Bioenergetics* 2010, *1797*, 1687–1695.

[69] Viotti, C., Kruger, F., Krebs, M., Neubert, C. et al., The endoplasmic reticulum is the main membrane source for biogenesis of the lytic vacuole in *Arabidopsis*. *Plant Cell* 2013, *25*, 3434–3449.

[70] Araki, Y., Gonzalez, E. L., V- and P-type Ca^{2+}-stimulated ATPases in a calcifying strain of *Pleurochrysis* sp. (Haptophyceae). *J. Phycol.* 1998, *34*, 79–88.

[71] Corstjens, P. L. A. M., Gonzalez, E. L., Effects of nitrogen and phosphorus availability on the expression of the coccolith-vesicle V-ATPase (subunit c) of *Pleurochrysis* (Haptophyta). *J. Phycol.* 2004, *40*, 82–87.

[72] Langhorst, M. F., Reuter, A., Stuermer, C. A. O., Scaffolding microdomains and beyond: the function of reggie/flotillin proteins. *Cell Mol. Life Sci.* 2005, *62*, 2228–2240.

[73] Morrow, I. C., Parton, R. G., Flotillins and the PHB domain protein family: rafts, worms and anaesthetics. *Traffic* 2005, *6*, 725–740.

[74] Browman, D. T., Resek, M. E., Zajchowski, L. D., Robbins, S. M., Erlin-1 and erlin-2 are novel members of the prohibitin family of proteins that define lipid-raft-like domains of the ER. *J. Cell Sci.* 2006, *119*, 3149–3160.

[75] Browman, D. T., Hoegg, M. B., Robbins, S. M., The SPFH domain-containing proteins: more than lipid raft markers. *Trends Cell Biol.* 2007, *17*, 394–402.

[76] Valenzuela, J., Mazurie, A., Carlson, R. P., Gerlach, R. et al., Potential role of multiple carbon fixation pathways during lipid accumulation in *Phaeodactylum tricornutum*. *Biotechnol. Biofuels.* 2012, *5*, 40.

[77] Peng, S. E., Chen, W. N. U., Chen, H. K., Lu, C. Y. et al., Lipid bodies in coral-dinoflagellate endosymbiosis: Proteomic and ultrastructural studies. *Proteomics* 2011, *11*, 3540–3555.

[78] Song, Z. H., Nes, W. D., Inactivation of soybean sterol 24-C-methyltransferase by elongated sterol side chains at C26. *Bioorg. Med. Chem. Lett.* 2007, *17*, 5902–5906.

[79] Gladu, P. K., Patterson, G. W., Wikfors, G. H., Chitwood, D. J. et al., The occurrence of brassicasterol and epibrassicasterol in the chromophycota. *Comp. Biochem. Phys. B* 1990, *97*, 491–494.

[80] Wojciech, Z. A., Goad, L. J., Goodwin, T. W., S-Adenosyl-L-methionine-cycloartenol methyltransferase activity in cell-free system from *Trebouxia* sp. and *Scenedesmus obliquus*. *Biochem. J.* 1973, *136*, 405–412.

[81] Not, F., Siano, R., Kooistra, W. H. C. F., Simon, N. et al., Diversity and ecology of eukaryotic marine phytoplankton. *Adv. Bot. Res. 2012*, *64*, 1–53.

[82] Dorrell, R. G., Smith, A. G., Do red and green make brown?: perspectives on plastid acquisitions within chromalveolates. *Eukaryot. Cell 2011*, *10*, 856–868.

